Published online 15 June 2010 *Nucleic Acids Research, 2010, Vol. 38, No. 19* ***6567–6576***
doi:10.1093/nar/gkq534

Intracellular delivery of an antisense oligonucleotide via endocytosis of a G protein-coupled receptor

Xin Ming[1], Md Rowshon Alam[1], Michael Fisher[1], Yongjun Yan[2], Xiaoyuan Chen[2] and Rudolph L. Juliano[1,*]

[1]Division of Molecular Pharmaceutics, UNC Eshelman School of Pharmacy, University of North Carolina, Chapel Hill, NC 27599 and [2]Laboratory of Molecular Imaging and Nanomedicine (LOMIN), National Institute of Biomedical Imaging and Bioengineering (NIBIB), National Institutes of Health, Bethesda, MD 20810, USA

Received March 4, 2010; Revised May 26, 2010; Accepted May 27, 2010

ABSTRACT

Gastrin-releasing peptide receptor (GRPR), a member of the G protein-coupled receptor superfamily, has been utilized for receptor-mediated targeting of imaging and therapeutic agents; here we extend its use to oligonucleotide delivery. A splice-shifting antisense oligonucleotide was conjugated to a bombesin (BBN) peptide, and its intracellular delivery was tested in GRPR expressing PC3 cells stably transfected with a luciferase gene interrupted by an abnormally spliced intron. The BBN-conjugate produced significantly higher luciferase expression compared to unmodified oligonucleotide, and this increase was reversed by excess BBN peptide. Kinetic studies revealed a combination of saturable, receptor-mediated endocytosis and non-saturable pinocytosis for uptake of the conjugate. The K_m value for saturable uptake was similar to the EC_{50} value for the pharmacological response, indicating that receptor-mediated endocytosis was a primary contributor to the response. Use of pharmacological and molecular inhibitors of endocytosis showed that the conjugate utilized a clathrin-, actin- and dynamin-dependent pathway to enter PC3 cells. The BBN-conjugate partially localized in endomembrane vesicles that were associated with Rab7 or Rab9, demonstrating that it was transported to late endosomes and the *trans*-golgi network. These observations suggest that the BBN-oligonucleotide conjugate enters cells via a process of GRPR mediated endocytosis followed by trafficking to deep endomembrane compartments.

INTRODUCTION

Oligonucleotide-based therapeutics has shown promise for treating a variety of diseases. New generations of antisense oligonucleotides provide better biological and pharmaceutical properties than conventional phosphorothioate oligonucleotides (1–4). Additionally, the discovery of mammalian RNA interference (RNAi) has enabled a new strategy for therapeutic regulation of gene expression (5,6). Promising results for both antisense and RNAi have been attained in cell culture and animal models, and this has driven the initiation of clinical trials. As of 2008, 17 US pharmaceutical industry sponsored clinical trials were ongoing with therapeutic oligonucleotides (http://www.phrma.org/). Despite these exciting prospects, a key hurdle impeding the wider success of this approach is poor delivery of oligonucleotides to their functional sites within cells, due to the need to cross several biological barriers subsequent to administration (7,8).

There are two major strategies to overcome biological barriers and allow successful delivery. One is to formulate oligonucleotides into nanoparticles with cationic lipids or polymers in order to improve intracellular uptake and endosomal release. This strategy has achieved significant success in cellular and animal studies (9–12); however, the large size and/or considerable toxicity of cationic lipid and polymer complexes may raise issues for clinical utilization (13). Another strategy is to utilize receptor-mediated targeting for pharmacologically effective delivery of antisense and siRNA oligonucleotides, in which a ligand that selectively binds to a cell surface receptor is chemically conjugated to the oligonucleotide (14). The potential advantages of this strategy are: (i) it will allow preferential delivery of the ligand–oligonucleotide conjugate to particular tissues and cell types in which the targeted receptor is differentially expressed; (ii) it may deliver the oligonucleotide to appropriate sites of action within cells;

*To whom correspondence should be addressed. Tel: +1 919 966 4383; Fax: +1 919 966 5640; Email: arjay@med.unc.edu

(iii) the small size of the ligand–oligonucleotide conjugates will allow ready egress from the blood and widespread distribution in tissues, which may be a significant advantage over various particulate oligonucleotide carriers in terms of *in vivo* pharmacokinetics, biodistribution and therapeutic effect.

Members of the integrin family of cell surface receptors have been utilized to deliver oligonucleotide conjugates (15,16), but evaluating additional types of receptors may contribute to the ultimate success of this approach (17). The G protein-coupled receptors (GPCRs) comprise the largest receptor family in the human genome with ~850 members (18). The conformational changes of GPCRs upon ligand occupancy lead to the dissociation of the α- and β/γ-subunits of the coupled G protein, thus triggering downstream effectors to produce changes in cell function, such as alteration of cAMP levels, activation of ion channels and activation of phospholipases (19). Regulation of the signaling activity of GPCRs involves processes of receptor internalization and recycling, which occur primarily through clathrin-mediated endocytosis (20). Once internalized, GPCRs can be sorted into various trafficking pathways including recycling to the cell surface, or degradation in lysosomes (21,22). Since clathrin mediated endocytosis is usually considered to be a high capacity pathway (23), this suggests that GPCRs may be suitable vehicles for efficient intracellular delivery of ligand–oligonucleotide conjugates.

Within GPCRs, bombesin (BBN) family receptors have been successfully used for receptor-mediated delivery of cytotoxins, immunotoxins and radioactive compounds (24,25). This family is composed of the neuromedin B receptor (NMBR) and gastrin-releasing peptide receptor (GRPR) sub-families (26). Over-expression of GRPRs has been implicated in breast, prostate, small cell lung, and pancreatic cancers (27). This has led to a substantial amount of work using BBN analogs to selectively deliver both imaging agents and conventional cytotoxic drugs to tumors (27,28). In the current study, this approach has been extended to delivery of oligonucleotides. The BBN peptide was coupled to a 'splice-shifting oligonucleotide' (SSO) designed to correct splicing of an aberrant intron inserted into the firefly luciferase reporter gene. Thus, successful delivery of the SSO to the cell nucleus would result in up-regulation of luciferase activity. This study showed that the BBN peptide can effectively deliver the SSO to GRPR positive cells in culture via a receptor-mediated endocytotic process. Preliminary mechanistic studies also delineated the endocytotic and intracellular trafficking pathways that may contribute to the effectiveness of the BBN–oligonucleotide conjugate.

MATERIALS AND METHODS

Synthesis and chemical characterization of peptide-oligonucleotide conjugates

The 2′-*O*-Me phosphorothioate oligonucleotide 623 (5′GTTATTCTTTAGAATGGTGC3′), its 3′-Tamra conjugate and 5′-thiol oligonucleotide, as well as the mismatched control (5′GTAATTATTTATAATCGTCC3′), were prepared as previously reported (15). In brief, oligonucleotides were synthesized using phosphoramidites of the ultraMILD-protected bases on 3′-Tamra CPG supports (Glen Research, Sterling, VA, USA) using a AB 3400 DNA synthesizer (Applied Biosystems, Foster City, CA, USA). To prepare peptide conjugates, a thiol linker was introduced at the 5′-end of the oligonucleotides. After cleavage from the CPG support and deprotection, the oligonucleotides were purified by reverse-phase HPLC on a Varian HPLC system (ProStar/Dynamax, Walnut Creek, CA, USA) and identified using matrix-assisted laser desorption ionization time-of-flight (MALDI–TOF) mass spectroscopy on a Voyager Applied Biosystem instrument (Foster City). The peptide BBN(6–14) was reacted with maleimide NHS ester in borate buffer at room temperature. Then, BBN–maleimide was isolated by semi-preparative HPLC and confirmed by MALDI–TOF. Thiol oligonucleotides were reacted with the maleimide-containing BBN peptide in a reaction buffer (final salt concentration adjusted to 400 mM KCl, 40% aqueous CH_3CN). The reaction mixture was vortexed and allowed to stand for 3 h, and purified by HPLC using a 1 ml Resource Q column (GE Healthcare, Uppsala, Sweden). The purified conjugates were dialyzed versus milli-Q water, and analyzed by MALDI–TOF.

Cell lines, plasmids and transfection

PC3 prostate cancer cells were cultured in F12K medium (Gibco/Invitrogen, Carlsbad, CA, USA) supplemented with 10% fetal bovine serum (FBS). The plasmid pLuc/705, containing an aberrant intron inserted into the firefly luciferase coding sequence was a kind gift from Dr R. Kole (University of North Carolina) (29). The Luc705 cassette was amplified from the plasmid pLuc/705 using the forward primer 5′TGCATGCTCGAGACATTTTACAATTTGG3′ and reverse primer 5′CCTGCAGGCATGCAAGCTTGGCATTCCG3′. Amplified PCR product was inserted at the *XhoI* and *HindIII* site of pcDNA3.1/hygro (Invitrogen) resulting in the plasmid pcDNA3.1/hygro/Luc705. Stable transfectants were obtained by transfecting PC3 cells with pcDNA3.1/hygro/Luc705 using Lipofectamine 2000® as per manufacturer's instructions. Selection was carried out in F12K medium containing 200 μg/ml hygromycin B (Roche) and 10% FBS for 2 weeks. Individual clones were picked and screened for luciferase induction by 623 oligonucleotide complexed with Lipofectamine 2000®. The single cell clone with the highest expression induced by 623 oligonucleotide was referred to as PC3/Luc705 and used in further studies.

A dynamin dominant negative (DN) expression plasmid was a kind gift from Dr JoAnn Trejo (University of California at San Diego, USA). The plasmids encoding eGFP-Rab5, eGFP-Rab7, eGFP-Rab9 and eGFP-Rab11 were kindly provided by Dr Stephen Ferguson (Robarts Research Institute, Canada), Prof. Bo van Deurs (University of Copenhagen, Denmark), Dr Suzanne Pfeffer (Stanford University, USA) and Dr Martin Alexander Schwartz (University of Virginia, USA), respectively. Plasmids expressing eGFP chimeras of dynamin or Rabs were transfected into the PC3/Luc705

cells. Briefly, 1 day after seeding in six-well plates, the cells were transfected with plasmids under serum free conditions in OPTI-MEM using Lipofectamine2000® as per manufacturer's instructions. Four hours later media was replaced with F12K supplemented with 10% FBS. The following day cells were treated with oligonucleotides, and uptake and intracellular distribution of the oligonucleotides were analyzed by flow cytometry and confocal microscopy, respectively.

Cellular uptake by flow cytometry

Total cellular uptake of the Tamra-labeled oligonucleotide was measured by flow cytometry using a LSR II cell analyzer (Becton-Dickenson, San Jose, CA, USA). After treatment with oligonucleotides for various times, the cells were trypsinized and analyzed by flow cytometry, with a 561 nm laser and a 582/15 emission filters for Tamra fluorescence, a 594 nm laser and a 610/20 emission filters for Alexa-594 fluorescence, and a 488 nm laser and a 525/50 filters for eGFP. For kinetic studies, varying amounts of the Tamra-labeled oligonucleotide were added to the culture medium to give increasing total substrate concentrations. Uptake was determined in the PC3/Luc705 cells over a 4-h period, which is within the linear uptake region. Kinetic constants (J_{max}, K_m and K_d) were obtained by fitting a model incorporating saturable and non-saturable components to the uptake data. The following model was utilized:

$$J = \frac{J_{max} \times C}{K_m + C} + K_d \times C \quad (1)$$

where J_{max} is the maximal uptake rate, K_m is the kinetic constant for saturable uptake, K_d is the kinetic constant for non-saturable uptake, and C is the oligonucleotide concentration. For inhibition studies, PC3/Luc705 cells were first treated with inhibitors for 30 min, and then the uptake of the conjugate was determined over a 4-h period in the presence of inhibitors. Alexa-594 labeled transferrin (Molecular Probes, Beaverton, OR, USA) was used as a control for clathrin-mediated endocytosis. After pretreatment with inhibitors in serum-free media, the cells were treated with 20 μg/ml transferrin for 15 min in the presence of the inhibitors, and then washed with acidic buffer to remove external transferrin. Flow cytometry was utilized to measure the uptake in both kinetic and inhibition studies.

Oligonucleotide treatment and luciferase assay

PC3/Luc705 cells were plated on 24-well plates (at 1.0×10^5 cells per well in various experiments) in F12K supplemented with 10% FBS. The following day, cells were treated with either free 623 oligonucleotide, 623 complexed with Lipofectamine 2000® as per manufacturer's instruction, BBN–623 conjugate, or its mismatched control prepared in OPTI-MEM I medium (Gibco). Four hours after treatment, 1% FBS was added to each well. Twenty-four hours after oligonucleotide treatment, medium was replaced with F12K containing 1% FBS, and at various times thereafter cell lysates were collected for luciferase assay. Cells were usually harvested 48 h after oligonucleotide treatment, or at times indicated in the figures. The expression of the firefly luciferase gene was measured by real-time RT–PCR as described below and the enzyme activity was determined using a Luciferase assay kit (Promega, Madison, WI, USA). Luciferase assay was performed on a FLUOstar Omega microplate reader (BMG LABTECH, Cary, NC, USA). Protein content was determined by the BCA protein assay (Pierce, Rockford, IL, USA) with bovine serum albumin as a standard. Background luciferase expression was determined by measuring luciferase activity in the cells without the oligonucleotide treatment, and these values were then subtracted from the results in the treated cells to obtain response values and the final dynamic data. In some cases, the effects of the BBN–623 conjugate were evaluated in the presence of free BBN peptide (Peptides International Inc, Louisville, KY, USA).

For pharmacodynamic studies, varying amounts of the BBN–623–Tamra were added to the culture medium to give increasing total substrate concentrations. Luciferase induction was determined in the PC3/Luc705 cells over a 24-h treatment followed by a 2-day culture. Pharmacodynamic constants (E_{max}, EC_{50} and γ) were obtained by fitting a general sigmoid model to the induction data. The following model was utilized:

$$E = \frac{E_{max} \times C^{\gamma}}{EC_{50}^{\gamma} + C^{\gamma}} \quad (2)$$

where E is the effect observed at the oligonucleotide concentration C, E_{max} is the maximal response that can be produced by the oligonucleotide, EC_{50} is the concentration of the drug that produces 50% of maximal effect, and γ is the Hill coefficient indicating the slope of the sigmoid curve.

RNA extraction and real-time RT–PCR

Total RNA was isolated using an RNeasy® Mini kit (Qiagen Inc., Valencia, CA, USA), and cDNA was synthesized from total RNA using an Enhanced Avian First Strand Synthesis Kit (Sigma, St Louis, MO, USA). The forward primer (5′CGATCCCTTCAGGATTACAAA3′), the reverse primer (5′GAGTGCTTTTGGCGAAGAAT3′), and the TaqMan® MGB probe (6FAM-TCAAAGTGCGTTGCTAGTACCAACCC-MGBNFQ) were designed based on firefly luciferase cDNA sequence using Primer3 software and were synthesized by Applied Biosystems (Foster City). The forward primer spans the insertion site of the aberrant intron 705 so that only correctly spliced luciferase mRNA can be amplified in the RT-PCR reaction. TaqMan® Human GAPDH Control Reagents (Applied Biosystems) were used for quantification of GAPDH in each sample and served as an internal control. Real-time PCR was performed using the ABI PRISM 7900 sequence detection system (Applied Biosystems). The luciferase expression levels of samples were calculated with the Comparative C_T Method ($\Delta\Delta C_T$ Method) and were expressed as fold changes over those of the non-treated cells.

Confocal fluorescence microscopy

Intracellular distribution of the oligonucleotide in living cells was examined using a Zeiss 510 Meta Inverted Laser Scanning Confocal Microscope with 63×-oil immersion objectives. PC3/Luc705 cells were plated in 35 mm glass bottom microwell dishes (MatTek, Ashland, MA, USA). After transfection of dynamin DN plasmid, intracellular uptake of the oligonucleotide, or of Alexa-594 labeled transferrin (Molecular Probes) as a marker for clathrin-coated vesicles, was visualized by confocal microscopy. Co-localization of the Tamra-labeled oligonucleotide with Alexa-488 labeled transferrin (Molecular Probes) was also done by confocal microscopy. Sub-cellular localization of BBN–623–Tamra in specific endomembrane compartments was performed by co-localization of the oligonucleotide with eGFP-Rab5 (early endosome marker), eGFP-Rab7 (late endosome marker), eGFP-Rab9 (*trans*-Golgi marker) and eGFP-Rab11 (recycling endosome marker), respectively, after expression of these plasmids in the cells.

Data analysis

Data are expressed as mean ± SD from three measurements unless otherwise noted. Statistical significance was evaluated using *t*-test or ANOVA followed by Dunnet's test for multiple comparisons. The data were analyzed with GraphPad Prism 5 (GraphPad Software, Inc., La Jolla, CA, USA). Parameter estimates were obtained by fitting the model to the cellular uptake and luciferase induction data using non-linear least-squares regression (WinNonlin, Pharsight, Mountain View, CA, USA). A weighting scheme of 1/Y and the Gauss–Newton (Levenberg and Hartley) minimization method were used for each modeling exercise.

RESULTS

Synthesis and characterization

The chemical structure of the final oligonucleotide conjugate is shown in Figure 1A. A Tamra fluorophore was introduced at the 3′-end of the oligonucleotide 623 or its mismatched control (5MM623). The BBN peptide (6–14) with maleimide functionality was coupled with the 5′-thiol oligonucleotides. After purification by ion-exchange chromatography, the identity of the final products were confirmed by MALDI–TOF mass spectroscopy (BBN–623–Tamra: calculated mass = 9129.3 $(M+H)^+$ and mass found = 9128.5 $(M+H)^+$; BBN-5MM623–Tamra: calculated mass = 9059.0 $(M+H)^+$ and mass found = 9059.6 $(M+H)^+$) (Figure 1B).

Cellular uptake and luciferase induction

The kinetics of total cellular uptake of 623–Tamra or its BBN–conjugate was evaluated by incubating cells with these molecules up to 24 h and then measuring total cell-associated fluorescence by flow cytometry. As seen in Figure 2A, there was at least a 2-fold greater uptake of the BBN–conjugate as compared to the unconjugated oligonucleotide at each time point. To evaluate pharmacological effects, free 623, the BBN–623 conjugate, the BBN-5MM623, and free 623 complexed with Lipofectamine 2000® (all 50 nM) were incubated with PC3/Luc705 cells and the cells were tested for luciferase expression by real-time RT–PCR (Figure 2B) and luciferase enzyme assay (Figure 2C). As seen in Figure 2B, the BBN–623 conjugate produced a significant increase in luciferase gene expression compared to the unconjugated 623 at the same concentration. Treatment of PC3/Luc705 cells with a mismatched oligonucleotide conjugated with BBN peptide failed to produce an increase in luciferase gene expression, indicating that the luciferase response depends on specific interaction of the 623 oligonucleotide with the splicing machinery in the nucleus. As seen in Figure 2C, the result from the luciferase assay confirmed that the BBN–623 conjugate generated a significantly higher luciferase activity compared to the free 623. To test whether the effect of the BBN–623 conjugate on splicing of the luciferase reporter was due to receptor-mediated endocytosis involving GRPR, excess amounts of full-length BBN peptide, a ligand that binds to the same site on the receptor, were used in the experiment. Co-incubation with 10 μM of this peptide led to full inhibition of the effect of the BBN–conjugate on luciferase expression (Figure 2C). This observation supports the concept that the effect of the BBN–conjugate on splicing largely depends on its initial uptake via GRPR. In addition, neither 623–Tamra oligonucleotide nor its BBN–conjugate showed toxicity at concentrations up to 1000 nM since the protein content of the treated cells was the same as the control when measured at the end of the induction experiment.

Dose–response studies of cellular uptake and biological effect

Cell uptake and pharmacological response for the BBN–conjugate were evaluated as a function of concentration. The initial uptake rate of the conjugate (at 37°C for 4 h) as a function of concentration was well described by a model consisting of one saturable and one non-saturable terms (Figure 3A). The J_{max} and K_m estimated for the saturable component were 2336 ± 454 FU/4 h and 122 ± 32 nM. The non-saturable component of uptake, K_d, was estimated to be 2.1 ± 0.4 FU/4h/nM. The K_m value is similar to the reported binding affinity of BBN to the GRPR, 79 nM (30). The data are consistent with a combination of a saturable, receptor-mediated endocytosis and non-saturable pinocytosis accounting for uptake of the conjugate in PC3 cells. The luciferase induction by the conjugate as a function of concentration was also saturable and well described by a general sigmoid model. The E_{max} and EC_{50} estimated for the response were 440 832 ± 75 734 LUs/μg protein and 97 ± 21 nM, respectively (Figure 3B). The EC_{50} value was similar to the K_m value for saturable uptake of the conjugate (122 ± 32 nM), which suggests that saturable, receptor-mediated endocytosis is the main contributor to the effectiveness of the conjugate.

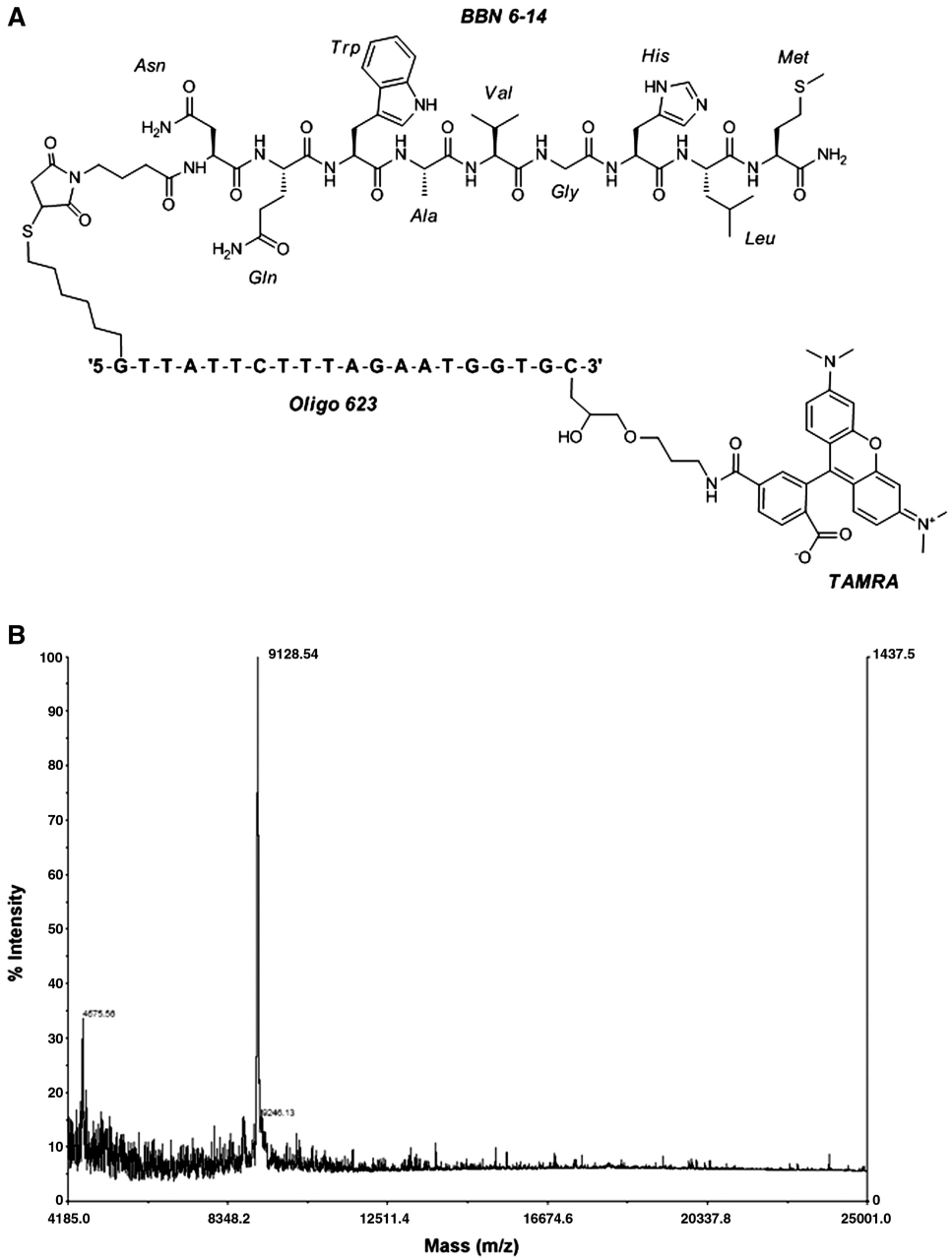

Figure 1. Chemical structure (**A**) and mass spectrum of the BBN–623 conjugate (**B**).

Time-response studies

The time-dependent response of luciferase to the BBN–623 conjugate was examined by harvesting the cells at various times after the period of exposure to the oligonucleotide. Figure 4 shows a striking difference between the time profiles of the responses induced by the BBN–623 conjugate and a cationic lipid/623 complex. The cationic lipid/623 was more effective than the BBN–conjugate showing a 2.6-fold higher AUC of the time-dependent response curve up to 96 h (Figure 4). The effect of the BBN–623 conjugate on luciferase expression rose gradually with time and reached a maximum at 72 h (48 h after removal of the oligonucleotide). In contrast, the effect of the cationic lipid/623 complex peaked at early time points after dosing and declined steadily thereafter. This difference may result from the different delivery mechanisms utilized by the receptor targeted conjugate and the cationic lipid complex. The oligonucleotide delivered via cationic lipids seems to reach the nucleus rapidly possibly due to quick endosomal release, while that delivered via the peptide-conjugate seems to traffic through other intracellular compartments and only gradually reach the nucleus where the effect on splicing takes place.

Uptake pathway

The effects of some known endocytosis inhibitors on the initial uptake rate of the BBN–conjugate were examined. Chlorpromazine is thought to interfere selectively with

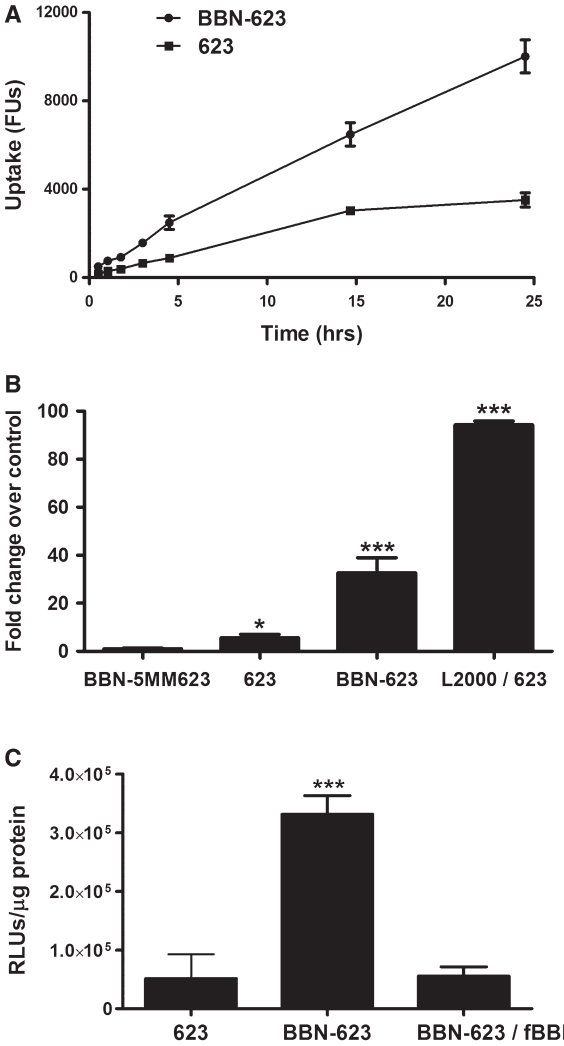

Figure 2. Cellular uptake kinetics (**A**) and luciferase induction measured by RT-PCR (**B**) and luciferase assay (**C**) for 623–Tamra and BBN–623–Tamra. (A) Cells in 24-well plates were treated with 50 nM of free 623–Tamra, or BBN–623–Tamra, for 0–24 h in OPTI-MEM at 37°C. The cells were rinsed in buffered saline solution and then trypsinized. Total cellular uptake of the Tamra-labeled oligonucleotide was measured by flow cytometry using a LSR II cell analyzer (Becton–Dickenson, San Jose, CA, USA). (B) Cells were treated with 623–Tamra, BBN–623–Tamra conjugate, or its mismatched control for 24 h, or with 623–Tamra complexed with Lipofectamine2000 for 4 h, as described in Materials and methods section, and luciferase gene expression was determined by real-time RT-PCR after 24 h for the liposomal complex or 48 h for the other treatments. (C) Cells were treated with either 623–Tamra, BBN–623–Tamra conjugate or BBN–623–Tamra in the presence of excess free BBN peptide (fBBN) for 24 h as described in 'Materials and Methods' section, and luciferase activity was determined after 48 h. Results are the means and standard deviations of triplicate determinations. $*P < 0.05$; $***P < 0.001$.

clathrin mediated endocytosis, while cytochalasin D blocks actin filament function, which is necessary for most forms of endocytosis (31). Both cytochalasin D (2 μM) and chlorpromazine (10 μM) inhibited the endocytosis of transferrin, a well-known marker for clathrin-mediated endocytosis (Figure 5); as well, both agents reduced the uptake of the BBN–623 conjugate. The inhibition studies supported the concept that the

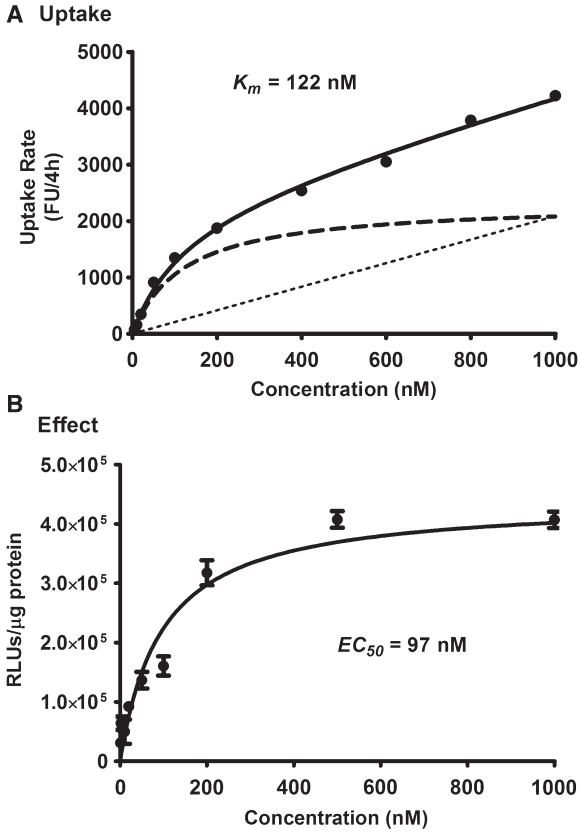

Figure 3. Dose-dependent initial cellular uptake (**A**) and response (**B**) for BBN–623–Tamra. A. Cells in 96-well plates were treated with increasing concentrations of BBN–623–Tamra, for 4 h in OPTI-MEM at 37°C. Then, the cells were rinsed in buffered saline solution and then trypsinized. Total cellular uptake of the Tamra-labeled oligonucleotide was measured by flow cytometry using a LSR II cell analyzer (Becton–Dickenson). The dashed line indicates the saturable component of uptake while the dotted line indicates non-saturable uptake. (B) Cells were treated with BBN–623–Tamra as described in 'Materials and Methods' section, and luciferase activity was determined after 48 h. Results are the means and standard deviations of triplicate determinations.

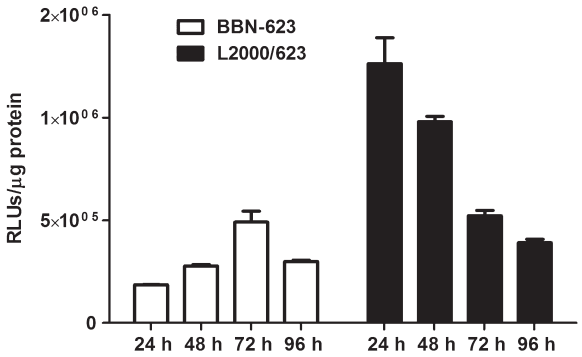

Figure 4. Time-dependent response studies. Cells were treated with either BBN–623–Tamra conjugate for 24 h or 623–Tamra complexed with Lipofectamine 2000® for 4 h, as described in 'Materials and Methods' section, and luciferase activity was determined at the times indicated after dosing. White bars represent luciferase activity of 50 nM BBN–623–Tamra conjugate and black bars represent 50 nM 623–Tamra complexed with Lipofectamine 2000®, all expressed as RLUs/μg protein. Results are the means and standard deviations of triplicate determinations.

BBN–oligonucleotide conjugate enters cells via clathrin-coated pits. Similar studies were done with methyl-β-cyclodextrin and amiloride that putatively inhibit lipid-raft mediated endocytosis and macropinocytosis, respectively. The lack of effect suggested that lipid-raft mediated vesicles are not involved in uptake of BBN–623, nor is macropinocytosis. However, since pharmacological inhibitors often have multiple effects we decided to further investigate the uptake and trafficking pathway of the conjugate.

Dynamin is a small GTPase that plays a key role in pinching off membrane vesicles and clathrin-dependent endocytotic pathways depend on the action of dynamin (32). The potential role of dynamin in oligonucleotide uptake in this system was examined by transfecting cells with plasmids coding for a chimeric protein comprised of a DN form of dynamin linked to eGFP. These cells were then treated with transferrin labeled with Alexa-594 or BBN–623–Tamra and observed for the extent of uptake and the subcellular distribution of the accumulated fluorescent molecules. As seen in Figure 6A, expression of high levels of DN-dynamin-eGFP almost completely blocked the accumulation of transferrin in intracellular vesicles, indicating that the function of dynamin is blocked in the transfected cells. The expression of DN-dynamin-eGFP also blocked the uptake of BBN–623–Tamra as observed in the confocal images. Flow cytometry can give a more quantitative assessment of the role of dynamin. After transfection, PC3 cells showed heterogeneous expression of mutant dynamin reflected by the pattern of eGFP expression in flow. In Figure 6B, the population of cells labeled in blue did not express DN-dynamin-eGFP and showed the same level of eGFP fluorescence as control cells, while the population labeled in purple showed high expression of DN-dynamin eGFP. Tamra fluorescence from the BBN–conjugate in the untransfected (blue) population was 1161 fluorescence units, while in the transfected (purple) population it was 385, a reduction of about 3-fold. This confirms that the uptake pathway for the BBN–623 oligonucleotide is dependent on dynamin function.

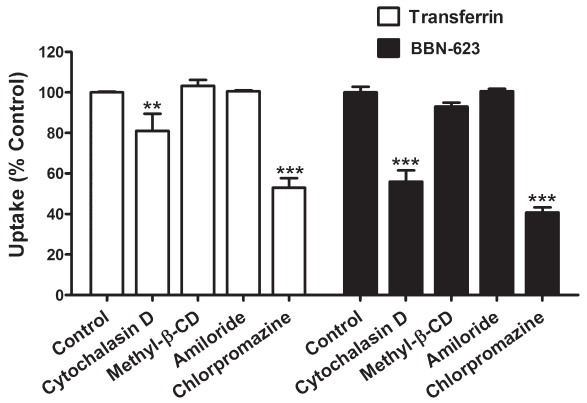

Figure 5. Effects of inhibitors on initial uptake of BBN–623–Tamra. Cells were treated with endocytosis inhibitors at the indicated concentrations for 30 min and then 20 μg/ml Alexa594-transferrin or 50 nM BBN–623–Tamra was added. After 15 min (transferrin) or 4 h (BBN–623–Tamra), the cells were rinsed in buffered saline solution and then trypsinized. Total cellular uptake was measured by flow cytometry using a LSR II cell analyzer (Becton–Dickenson). Results represent means and standard deviations of triplicate determinations and are normalized based on cells receiving no inhibitor as 100%. $^{**}P < 0.01$; $^{***}P < 0.001$.

Subcellular distribution

The colocalization of the BBN–623 conjugate with Alexa-488 labeled transferrin, a marker for clathrin-coated vesicle endocytosis, was examined in live cells. After treatment for 2 h, there was partial co-localization of the BBN–conjugate with transferrin (Figure 7A), suggesting the BBN–oligonucleotide conjugate initially enters cells via a clathrin-mediated endocytic process that is shared by transferrin. To further pursue the subcellular fate of the BBN–conjugate we examined its distribution as compared to well-known markers for several endomembrane compartments. Rab small GTPases, members of the Ras superfamily, are localized at distinct membrane vesicles and are responsible for membrane vesicle formation, development and trafficking (33). Rab5, which is mainly localized to early endosomes, mediates endocytosis and endosome fusion (34). Rab11 mediates slow return of receptors to the plasma membrane through recycling endosomes (35). The late endosome-associated Rab7 mediates maturation of late endosomes and their fusion with lysosomes (36), whereas another late endosomal GTPase, Rab9, mediates trafficking between late endosomes and the *trans*-golgi network (TGN) (37). PC3 cells were transiently transfected with eGFP chimeras of these four Rabs, and subsequently the trafficking of the BBN–623–Tamra in live cells was examined by confocal microscopy of live cells. As shown in Figure 7B, after 4-h treatment, vesicles containing the conjugate were observed to colocalize with Rab7 or Rab9, indicating that BBN–623 was transported to late endosomes and the TGN. However, colocalization was not observed between the BBN–conjugate and Rab5 or Rab11 containing vesicles at both early and late time points (1 and 4 h) (data not shown). 3D reconstructions of the subcellular distribution of BBN–623 and the eGFP-Rab proteins are shown in Supplementary Figure S1, confirming the intracellular localization of the moieties displaying co-localization of the Rabs and oligonucleotides.

DISCUSSION

Targeting GPCRs shows promise for receptor mediated delivery of oligonucleotides. The GPCRs comprise the largest receptor family in the human genome (18). Individual members of this family often display differential expression in various tissues or between tumor and normal tissue (25,38,39). Therefore, ligand–oligonucleotide conjugates that bind a specific GPCR member can potentially lead to targeted delivery to a particular tissue. In addition, internalization and recycling of GPCRs occurs primarily through clathrin mediated endocytosis (20), which is usually considered to be a high capacity pathway (23). This suggests that GPCRs may be suitable vehicles for efficient intracellular delivery of

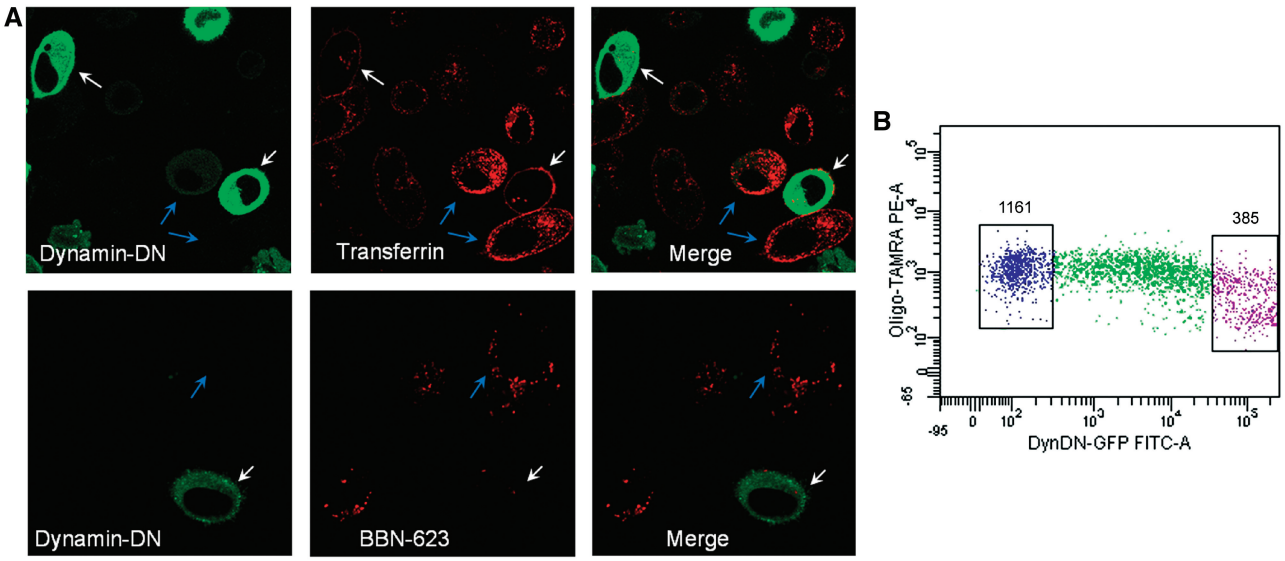

Figure 6. Effects of DN dynamin on cellular uptake of BBN–623–Tamra. The potential role of dynamin in BBN–623–Tamra uptake was examined by transfecting PC3 cells with a plasmid coding for DN-dynamin-eGFP. These cells were then treated with transferrin-Alexa-594 (20 μg/ml) or the BBN–623–Tamra conjugate (50 nM) and observed by confocal microscopy for the extent and subcellular distribution of the accumulated fluorescent molecules. Additionally total cell uptake was quantitated by flow cytometry. In (**A**) cells expressing high levels of DN-dynamin-eGFP are marked with white arrows while untransfected or poorly transfected cells are marked with blue arrows. As seen, expression of high levels of DN-dynamin-eGFP almost completely blocked the accumulation of transferrin in intracellular vesicles, indicating that the DN-dynamin-eGFP construct is functional. The expression of DN-dynamin-eGFP also blocked the uptake of BBN–623–Tamra, as seen in the confocal images, and also in the results from the flow cytometry (Figure 6B). There an approximate 3-fold reduction in total uptake was observed at high levels of eGFP-DN dynamin (purple dots) versus untransfected cells (blue dots). In (**B**) the abscissa is the expression of DN-dynamin-eGFP while the ordinate is uptake of BBN–623–Tamra.

ligand–oligonucleotide conjugates. GRPR is a tumor-related growth factor receptor whose expression has been detected in a large spectrum of human cancers, with high levels found in prostate, gastrinoma, breast and ovarian tumors (27). Thus, it has been considered as a promising target for therapeutic interventions and tumor detection. GRPR ligands have been extensively utilized to target cytotoxins, immunotoxins and radioactive compounds, and several of them have achieved clinical success. Several studies have shown that radiolabeled BBN peptides are suitable for detecting GRPR-positive prostate cancer *in vivo* with PET imaging (40–42). A BBN-derived, 99mTc-labeled pentadecapeptide showed significant uptake in tumor tissues, including breast cancer and prostate cancer, in pilot clinical studies (43). BBN analogs have also been linked to several cytotoxic agents for delivering these small molecule drugs in cancer treatment. AN-215, a conjugate of 2-pyrrolinodoxorubicin and BBN peptide, has been studied for almost a decade in many types of cancer, and been recently used as single and combined therapy in experimental ovarian cancers (44). In addition, conjugation of paclitaxel with BBN peptide enhanced cytotoxicity against human non-small-cell lung cancer compared with unconjugated taxol (45).

In the current study, a splicing switching oligonucleotide was conjugated to a BBN peptide. This conjugate showed higher cellular uptake in GRPR expressing cells, and intracellular delivery of this conjugate also produced an enhanced pharmacological response in terms of splicing correction, which was abolished by the presence of excess BBN peptide. For the first time, this study showed that targeting GRPR also can be utilized for selective intracellular delivery of oligonucleotides.

Use of selective endocytosis inhibitors and transfection with a DN mutant dynamin showed that the BBN–623 conjugate utilized a clathrin-dependent, actin-dependent and dynamin-dependent pathway to enter PC3 cells. Accordingly, modeling of the dose-dependent uptake data for BBN–623 revealed a combination of a major saturable component, likely receptor-mediated endocytosis and a minor non-saturable component, likely fluid phase pinocytosis, for uptake of the conjugate. In addition, the K_m value for saturable uptake of the conjugate was quite similar to the EC_{50} value for the pharmacological response. The pharmacodynamics of a splice switching oligonucleotide is complicated even in a cell-based model. The dose–response relationship depends on the cellular uptake, intracellular trafficking to nucleus, and the interaction of the oligonucleotide with the splicing machinery the nucleus. However, the similarity of the K_m value for saturable uptake of the conjugate and the EC_{50} value for the pharmacological response favors the notion that it is the saturable, receptor-mediated component of endocytosis that mainly contributes to the effectiveness of the conjugate.

Initial uptake of oligonucleotides is followed by sequential intracellular trafficking into a variety of endomembrane compartments. Intracellular trafficking can be rate-limiting because non-productive pathways can circumvent the transport of oligonucleotides to the target; for example, sorting to lysosomal vesicles may lead to

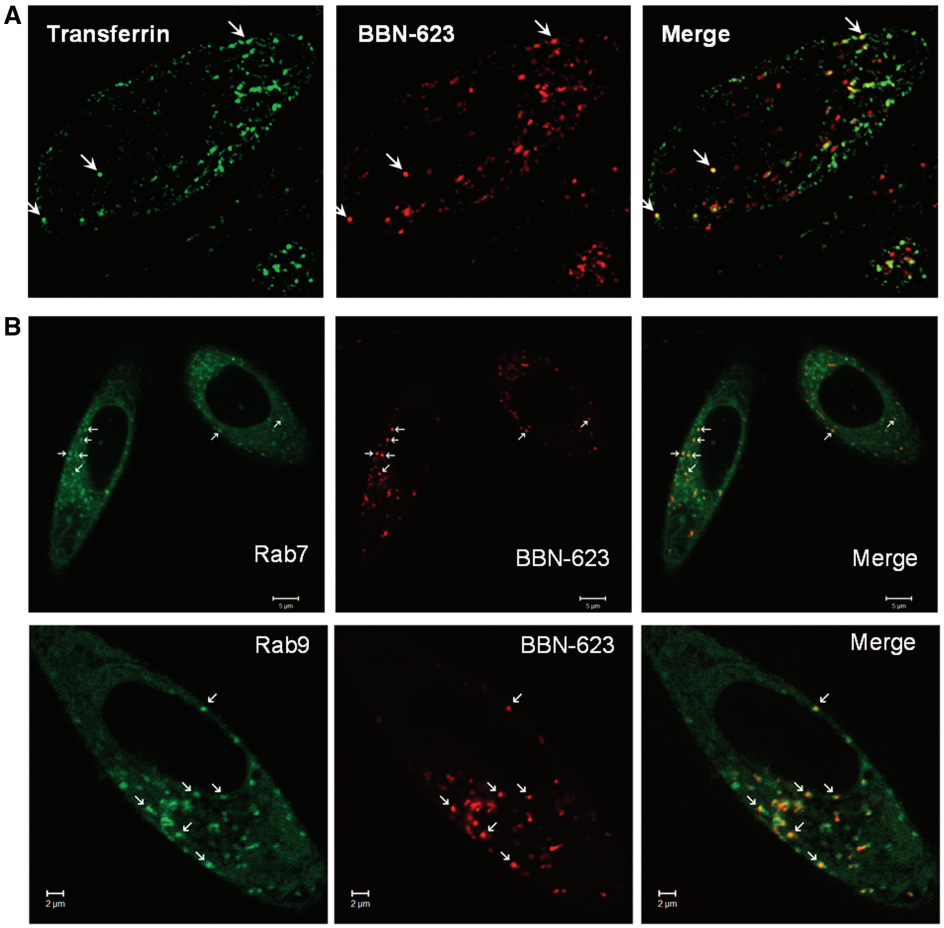

Figure 7. Co-localization with the endosomal pathway marker transferrin (**A**) and markers of endomembrane compartments (**B**). (A) BBN–623–Tamra oligonucleotide conjugate (50 nM) was co-incubated with Transferrin-Alexa 488 (10 μg/ml) for 2 h. Live cells were observed by confocal fluorescence microscopy as described in 'Materials and Methods' section. Selected vesicles showing co-localization (yellow) are marked with white arrows. (B) After transfecting PC3 cells with plasmids encoding eGFP-Rab7 (late endosome marker) and eGFP-Rab9 (*trans*-Golgi marker), respectively, cells were treated with 50 nM BBN–623–Tamra for 4 h. Live cells were observed by confocal fluorescence microscopy as described in the 'Materials and Methods' section. Selected vesicles showing co-localization (yellow) are marked with white arrows.

degradation. In this study, we observed that the BBN–623 conjugate was partially transported to late endosomes and to the TGN. This route may represent a productive pathway because it may bypass lysosomal degradation. However, the current data cannot delineate a complete picture of the trafficking from the TGN to the nucleus. The relatively slow action of the conjugate in inducing luciferase suggests that entry into the nucleus may occur at a slow rate. In conclusion, this study has generated a novel construct for intracellular delivery of oligonucleotides via GPCR-mediated endocytosis, and has made an initial examination of the endocytosis and intracellular trafficking pathways that may contribute to the effectiveness of this construct.

SUPPLEMENTARY DATA

Supplementary Data are available at NAR Online.

ACKNOWLEDGEMENTS

The authors gratefully acknowledge Dr JoAnn Trejo (University of California at San Diego, USA), Dr Stephen Ferguson (Robarts Research Institute, Canada), Prof. Bo van Deurs (University of Copenhagen, Denmark), Dr Suzanne Pfeffer (Stanford University, USA) and Dr Martin Alexander Schwartz (University of Virginia, USA) for providing the plasmids encoding eGFP-DN-dynamin, eGFP-Rab5, eGFP-Rab7, eGFP-Rab9 and eGFP-Rab11, respectively.

FUNDING

Grant P01GM059299 to R.L.J. Funding for open access charge: National Institutes of Health (grant P01GM059299).

Conflict of interest statement. None declared.

REFERENCES

1. Prakash,T.P. and Bhat,B. (2007) 2′-Modified oligonucleotides for antisense therapeutics. *Curr. Top. Med. Chem.*, **7**, 641–649.
2. Bennett,C.F. and Swayze,E.E. (2010) RNA targeting therapeutics: molecular mechanisms of antisense oligonucleotides as a therapeutic platform. *Annu. Rev. Pharmacol. Toxicol.*, **50**, 259–293.

3. Debart,F., Abes,S., Deglane,G., Moulton,H.M., Clair,P., Gait,M.J., Vasseur,J.J. and Lebleu,B. (2007) Chemical modifications to improve the cellular uptake of oligonucleotides. *Curr. Top. Med. Chem.*, **7**, 727–737.
4. Corey,D.R. (2007) Chemical modification: the key to clinical application of RNA interference? *J. Clin. Invest.*, **117**, 3615–3622.
5. McManus,M.T. and Sharp,P.A. (2002) Gene silencing in mammals by small interfering RNAs. *Nat. Rev. Genet.*, **3**, 737–747.
6. Castanotto,D. and Rossi,J.J. (2009) The promises and pitfalls of RNA-interference-based therapeutics. *Nature*, **457**, 426–433.
7. Juliano,R., Bauman,J., Kang,H. and Ming,X. (2009) Biological barriers to therapy with antisense and siRNA oligonucleotides. *Mol. Pharm.*, **6**, 686–695.
8. Whitehead,K.A., Langer,R. and Anderson,D.G. (2009) Knocking down barriers: advances in siRNA delivery. *Nat. Rev. Drug Discov.*, **8**, 129–138.
9. Gao,K. and Huang,L. (2009) Nonviral methods for siRNA delivery. *Mol. Pharm.*, **6**, 651–658.
10. Wu,S.Y. and McMillan,N.A. (2009) Lipidic systems for in vivo siRNA delivery. *AAPS J.*, **11**, 639–652.
11. Zimmermann,T.S., Lee,A.C., Akinc,A., Bramlage,B., Bumcrot,D., Fedoruk,M.N., Harborth,J., Heyes,J.A., Jeffs,L.B., John,M. *et al.* (2006) RNAi-mediated gene silencing in non-human primates. *Nature*, **441**, 111–114.
12. Frank-Kamenetsky,M., Grefhorst,A., Anderson,N.N., Racie,T.S., Bramlage,B., Akinc,A., Butler,D., Charisse,K., Dorkin,R., Fan,Y. *et al.* (2008) Therapeutic RNAi targeting PCSK9 acutely lowers plasma cholesterol in rodents and LDL cholesterol in nonhuman primates. *Proc. Natl Acad. Sci. USA*, **105**, 11915–11920.
13. Lv,H., Zhang,S., Wang,B., Cui,S. and Yan,J. (2006) Toxicity of cationic lipids and cationic polymers in gene delivery. *J. Control Release*, **114**, 100–109.
14. Juliano,R., Alam,M.R., Dixit,V. and Kang,H. (2008) Mechanisms and strategies for effective delivery of antisense and siRNA oligonucleotides. *Nucleic Acids Res.*, **36**, 4158–4171.
15. Alam,M.R., Dixit,V., Kang,H., Li,Z.B., Chen,X., Trejo,J., Fisher,M. and Juliano,R.L. (2008) Intracellular delivery of an anionic antisense oligonucleotide via receptor-mediated endocytosis. *Nucleic Acids Res.*, **36**, 2764–2776.
16. Alam,M.R., Ming,X., Dixit,V., Fisher,M., Chen,X. and Juliano,R.L. (2010) The biological effect of an antisense oligonucleotide depends on its route of endocytosis and trafficking. *Oligonucleotides*, **20**, 103–109.
17. Cesarone,G., Edupuganti,O.P., Chen,C.P. and Wickstrom,E. (2007) Insulin receptor substrate 1 knockdown in human MCF7 ER+ breast cancer cells by nuclease-resistant IRS1 siRNA conjugated to a disulfide-bridged D-peptide analogue of insulin-like growth factor 1. *Bioconjug. Chem.*, **18**, 1831–1840.
18. Armbruster,B.N. and Roth,B.L. (2005) Mining the receptorome. *J. Biol. Chem.*, **280**, 5129–5132.
19. Gilman,A.G. (1995) Nobel lecture. G proteins and regulation of adenylyl cyclase. *Biosci. Rep.*, **15**, 65–97.
20. Drake,M.T., Shenoy,S.K. and Lefkowitz,R.J. (2006) Trafficking of G protein-coupled receptors. *Circ. Res.*, **99**, 570–582.
21. Gaborik,Z. and Hunyady,L. (2004) Intracellular trafficking of hormone receptors. *Trends Endocrinol. Metab.*, **15**, 286–293.
22. Hanyaloglu,A.C. and von Zastrow,M. (2008) Regulation of GPCRs by endocytic membrane trafficking and its potential implications. *Annu. Rev. Pharmacol. Toxicol.*, **48**, 537–568.
23. Wolfe,B.L. and Trejo,J. (2007) Clathrin-dependent mechanisms of G protein-coupled receptor endocytosis. *Traffic*, **8**, 462–470.
24. Ananias,H.J., de Jong,I.J., Dierckx,R.A., van de Wiele,C., Helfrich,W. and Elsinga,P.H. (2008) Nuclear imaging of prostate cancer with gastrin-releasing-peptide-receptor targeted radiopharmaceuticals. *Curr. Pharm. Des.*, **14**, 3033–3047.
25. Cornelio,D.B., Roesler,R. and Schwartsmann,G. (2007) Gastrin-releasing peptide receptor as a molecular target in experimental anticancer therapy. *Ann. Oncol.*, **18**, 1457–1466.
26. Jensen,R.T., Battey,J.F., Spindel,E.R. and Benya,R.V. (2008) International Union of Pharmacology. LXVIII. Mammalian bombesin receptors: nomenclature, distribution, pharmacology, signaling, and functions in normal and disease states. *Pharmacol. Rev*, **60**, 1–42.
27. Smith,C.J., Volkert,W.A. and Hoffman,T.J. (2005) Radiolabeled peptide conjugates for targeting of the bombesin receptor superfamily subtypes. *Nucl. Med. Biol.*, **32**, 733–740.
28. Engel,J.B., Schally,A.V., Dietl,J., Rieger,L. and Honig,A. (2007) Targeted therapy of breast and gynecological cancers with cytotoxic analogues of peptide hormones. *Mol. Pharm.*, **4**, 652–658.
29. Kang,S.H., Cho,M.J. and Kole,R. (1998) Up-regulation of luciferase gene expression with antisense oligonucleotides: implications and applications in functional assay development. *Biochemistry*, **37**, 6235–6239.
30. Liu,Z., Yan,Y., Chin,F.T., Wang,F. and Chen,X. (2009) Dual integrin and gastrin-releasing peptide receptor targeted tumor imaging using 18F-labeled PEGylated RGD-bombesin heterodimer 18F-FB-PEG3-Glu-RGD-BBN. *J. Med. Chem.*, **52**, 425–432.
31. Khalil,I.A., Kogure,K., Akita,H. and Harashima,H. (2006) Uptake pathways and subsequent intracellular trafficking in nonviral gene delivery. *Pharmacol. Rev.*, **58**, 32–45.
32. Robinson,M.S. (1994) The role of clathrin, adaptors and dynamin in endocytosis. *Curr. Opin. Cell Biol.*, **6**, 538–544.
33. Stenmark,H. (2009) Rab GTPases as coordinators of vesicle traffic. *Nat. Rev. Mol. Cell Biol.*, **10**, 513–525.
34. Bucci,C., Lutcke,A., Steele-Mortimer,O., Olkkonen,V.M., Dupree,P., Chiariello,M., Bruni,C.B., Simons,K. and Zerial,M. (1995) Co-operative regulation of endocytosis by three Rab5 isoforms. *FEBS Lett.*, **366**, 65–71.
35. Ullrich,O., Reinsch,S., Urbe,S., Zerial,M. and Parton,R.G. (1996) Rab11 regulates recycling through the pericentriolar recycling endosome. *J. Cell Biol.*, **135**, 913–924.
36. Bucci,C., Thomsen,P., Nicoziani,P., McCarthy,J. and van Deurs,B. (2000) Rab7: a key to lysosome biogenesis. *Mol. Biol. Cell.*, **11**, 467–480.
37. Lombardi,D., Soldati,T., Riederer,M.A., Goda,Y., Zerial,M. and Pfeffer,S.R. (1993) Rab9 functions in transport between late endosomes and the trans golgi network. *EMBO J.*, **12**, 677–682.
38. Wu,X., Lee,V.C., Chevalier,E. and Hwang,S.T. (2009) Chemokine receptors as targets for cancer therapy. *Curr. Pharm. Des.*, **15**, 742–757.
39. Li,S., Huang,S. and Peng,S.B. (2005) Overexpression of G protein-coupled receptors in cancer cells: involvement in tumor progression. *Int. J. Oncol.*, **27**, 1329–1339.
40. Zhang,X., Cai,W., Cao,F., Schreibmann,E., Wu,Y., Wu,J.C., Xing,L. and Chen,X. (2006) 18F-labeled bombesin analogs for targeting GRP receptor-expressing prostate cancer. *J. Nucl. Med.*, **47**, 492–501.
41. Yang,Y.S., Zhang,X., Xiong,Z. and Chen,X. (2006) Comparative in vitro and in vivo evaluation of two 64Cu-labeled bombesin analogs in a mouse model of human prostate adenocarcinoma. *Nucl. Med. Biol.*, **33**, 371–380.
42. Chen,X., Park,R., Hou,Y., Tohme,M., Shahinian,A.H., Bading,J.R. and Conti,P.S. (2004) microPET and autoradiographic imaging of GRP receptor expression with 64Cu-DOTA-[Lys3]bombesin in human prostate adenocarcinoma xenografts. *J. Nucl. Med.*, **45**, 1390–1397.
43. Varvarigou,A., Bouziotis,P., Zikos,C., Scopinaro,F. and De Vincentis,G. (2004) Gastrin-releasing peptide (GRP) analogues for cancer imaging. *Cancer Biother. Radiopharm.*, **19**, 219–229.
44. Nagy,A. and Schally,A.V. (2005) Targeting cytotoxic conjugates of somatostatin, luteinizing hormone-releasing hormone and bombesin to cancers expressing their receptors: a "smarter" chemotherapy. *Curr. Pharm. Des.*, **11**, 1167–1180.
45. Safavy,A., Bonner,J.A., Waksal,H.W., Buchsbaum,D.J., Gillespie,G.Y., Khazaeli,M.B., Arani,R., Chen,D.T., Carpenter,M. and Raisch,K.P. (2003) Synthesis and biological evaluation of paclitaxel-C225 conjugate as a model for targeted drug delivery. *Bioconjugate Chem.*, **14**, 302–310.